THE JOURNAL OF PHYSICAL CHEMISTRY LETTERS
A JOURNAL OF THE AMERICAN CHEMICAL SOCIETY

Letter

The Hidden Path to the Resonance-Stabilized Fulvenallenyl Radical (C_7H_5) via the Bimolecular Reaction of Tricarbon (C_3, $X^1\Sigma_g^+$) with 1,3-Butadiene (C_4H_6; X^1A_g)

Iakov A. Medvedkov, Alexander M. Mebel,* Anatoliy A. Nikolayev, Zhenghai Yang, Shane J. Goettl, and Ralf I. Kaiser*

Cite This: *J. Phys. Chem. Lett.* 2026, 17, 2942−2952

Read Online

ACCESS | Metrics & More | Article Recommendations | Supporting Information

ABSTRACT: We report a novel bimolecular reaction pathway forming the resonance-stabilized fulvenallenyl radical (C_7H_5) *via* the gas-phase reaction of tricarbon (C_3, $X^1\Sigma g^+$) with 1,3-butadiene (C_4H_6, X^1A_g). Crossed molecular beam experiments combined with high-level electronic structures and statistical calculations reveal a rich potential energy surface. The reaction proceeds *via* tricarbon addition to a double bond of 1,3-butadiene, overcoming a 30 kJ mol^{-1} barrier, followed by ring closure, isomerizations (ring opening/closures, hydrogen shifts), and eventual hydrogen atom loss, yielding the fulvenallenyl radical (**p1**) almost exclusively via two dominant pathways. Considering the entrance barrier, this reaction may occur in high-temperature environments, like circumstellar envelopes of carbon stars, but is suppressed in colder regions such as molecular clouds and Titan's atmosphere. These findings highlight the unexpected reactivity of small carbon clusters in shaping the molecular complexity of our universe, from the flicker of a flame to the death of a star.

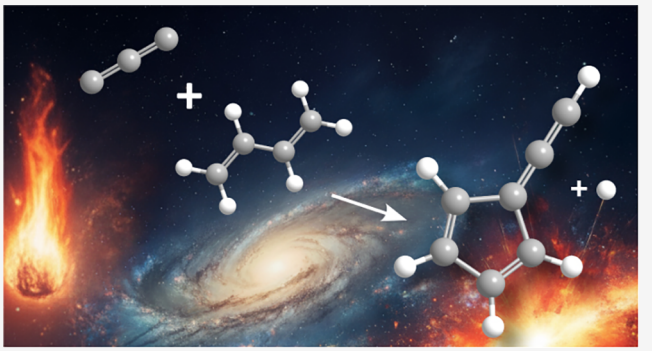

Despite over a century of intensive exploration in organic chemistry, the fulvenallenyl radical (C_7H_5) was only proposed in 2009[1] and experimentally detected in the laboratory in 2011 by using threshold photoionization mass spectrometry.[2,3] The C_7H_5 family encompasses a diverse array of cyclic (***1***, ***4***), bicyclic (***2***, ***3***), and acyclic (***5***,***6***) radicals comprising five-, six-, and seven-membered rings, with the fulvenallenyl radical (***1***) holding the global minima on the potential energy surface (Scheme 1).[4] This exceptional stability arises from significant resonance stabilization attributed to its propargyl- and cyclopentadienyl-like structures (Scheme 1). These hydrogen-deficient resonantly stabilized free radicals (RSFRs) are key intermediates for molecular mass growth processes in oxygen-deficient environments such as combustion flames,[5-10] extraterrestrial environments like carbon-rich circumstellar envelopes of, e.g., IRC+10216,[11-18] and the chemical vapor deposition process (CVD).[19] Here, their unique stability and chemistry drive the chemical evolution, yielding polycyclic aromatic hydrocarbons (PAHs) and, in turn, carbonaceous nanoparticles (including soot and interstellar and circumstellar dust) or fullerene structures such as C_{60} and C_{70}. The belated identification and growing significance of the fulvenallenyl chemistry[1,4,20-22] highlight that RSFRs continue to expose unexpected surprises that reshape our understanding of complex chemical systems that drive the molecular evolution of carbon in our Galaxy.

RSFRs, hydrogen-deficient carbon-bearing radicals stabilized by electron delocalization over multiple carbon atoms, are prepared through two main types of chemical processes. The first involves breaking a simple bond in closed-shell molecules via carbon−hydrogen (C−H) bond dissociation, hydrogen abstraction, and carbon-carbon (C-C) β-scission, either thermally or photolytically. The second involves forming at least one new bond during the reaction pathway, leading to RSFR generation via bimolecular gas-phase reactions. The most illustrative reactions in this class are those involving bare carbon clusters like atomic carbon (C), dicarbon (C_2), and tricarbon (C_3) with unsaturated hydrocarbons (Scheme 2).[12,15,23-25] These carbon clusters were also revealed as key structural building blocks for the molecular mass growth mechanisms in carbon-rich environments—including combustion flames, cold molecular clouds, carbon-rich stars, and CVD processes—to larger, often hydrogen-deficient carbon clusters, PAHs,[25-29] and fullerenes. It is important that while atomic

Published: January 29, 2026

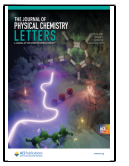

Scheme 1. Different C_7H_5 Isomers with the Enthalpy of Formation Relative to the Most Stable Isomer 1[a]

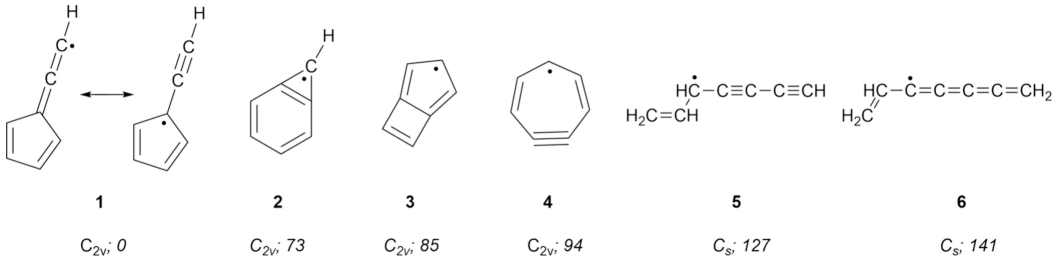

[a]Relative energies (kJ mol^{-1}) for **2**–**4** were taken from ref 4 and for **5**–**6** from current work.

Scheme 2. Resonantly Stabilized Free Radicals Synthesized in Bimolecular Reactions of Bare Carbon Clusters with Unsaturated Hydrocarbons

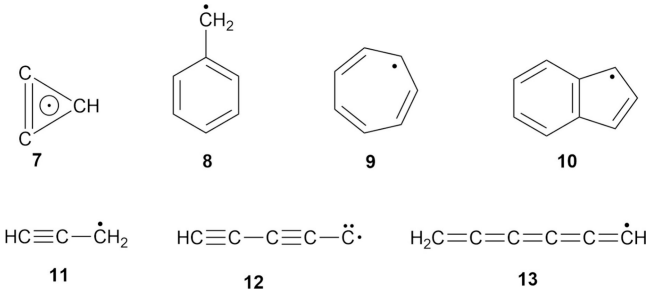

carbon $C(^3P)$[12,13,23,30-33] and dicarbon $C_2(X^1\Sigma_g^+/a^3\Pi_u)$[24,34-44] reactions usually form RSFRs via barrierless and overall exoergic pathways, thus operating even in energy-deficient environments like cold molecular clouds at 10 K, reactions of ground state tricarbon $C_3(X^1\Sigma_g^+)$[25,45-47] with unsaturated hydrocarbons demonstrate the opposite feature and the presence of an energy threshold of 30–50 kJ mol^{-1}, which effectively shut the door to the role of the hydrocarbon chemistry of tricarbon molecules in cold astrochemical environments, while still being feasible in high-temperature environments.

Considering the preparation of C_7H_5 radicals, dominating attention has been directed toward the unimolecular processes of the first type via C–H bond cleavage in fulvenallene (C_7H_6) at high temperatures[48] or *via* photolysis at 193 and 248 nm.[49,50] In contrast, bimolecular reaction pathways have remained unexplored. Only reaction 1[51-54] was studied theoretically and experimentally. This reaction was found to yield 2,6-cycloheptadien-4-yn-1-yl (**4**; Scheme 1) with no accessible pathway to fulvenallenyl. Alternative radical reactions 2–4[4,55] access C_7H_5 radicals only via three-body collision conditions as the radicals emerge from initial adducts and their isomerization processes and hence are irrelevant to the chemistry of cold molecular clouds like Taurus molecular cloud (TMC-1) where bimolecular reactions operate. The radical–radical reaction 5 should also be mentioned; although the low concentrations of radicals relative to closed-shell species pose a limitation, this pathway is expected to produce fulvenallenyl with a nearly 100% yield.

$$C\left(^3P_j\right) + C_6H_6\left(X^1A_{1g}\right) \rightarrow C_7H_5 + H \quad (1)$$

$$C_3H_3 + C_4H_2 + M \rightarrow C_7H_5 + M^* \quad (2)$$

$$C_2H_2 + i\text{-}C_5H_3 + M \rightarrow C_7H_5 + M^* \quad (3)$$

$$C_2H_2 + n\text{-}C_5H_3 + M \rightarrow C_7H_5 + M^* \quad (4)$$

$$i\text{-}C_3H_3 + i\text{-}C_4H_3 \rightarrow C_7H_5 + H \quad (5)$$

Here, we report the very first route leading to the formation of C_7H_5 isomers—among them the resonantly stabilized fulvenallenyl radical—shedding light on their origin in chemical systems via bimolecular reactions with astrophysically abundant, acyclic reactants by combining crossed molecular beam experiments with *ab initio* and statistical calculations of the reaction of ground state tricarbon (C_3, $X^1\Sigma_g^+$) with 1,3-butadiene (C_4H_6; X^1A_g).

Reactive scattering signal for the reaction of tricarbon (C_3; 36 amu) with 1,3-butadiene (C_4H_6; 54 amu) was monitored at the mass-to-charge (m/z) ratios of m/z = 89 ($C_7H_5^+$) and m/z = 88 ($C_7H_4^+$) for the atomic hydrogen (reaction 6) and/or molecular hydrogen loss pathways (reaction 7). No signal was detected at m/z = 88, indicating the presence of only an atomic hydrogen loss channel (reaction 6), leading to the formation of exclusively the C_7H_5 product (Figure S1). Hence, the corresponding TOF spectra of the reaction of tricarbon with 1,3-butadiene were collected at m/z = 89 and were then normalized to the signal at the CM angle to obtain the laboratory angular distribution (LAD) (Figure 1a) with a width of at least 30° and asymmetry around the CM angle of 30 ± 2°. The results suggest that the observed C_7H_5 products originate from indirect scattering dynamics, proceeding through transient complex formation that involves one or more C_7H_6 intermediates.[12,18,56]

$$C_3\ (36\ amu) + CH_2CHCHCH_2\ (54\ amu) \rightarrow C_7H_5\ (89\ amu) + H\ (1\ amu) \quad (6)$$

$$C_3(36\ amu) + CH_2CHCHCH_2\ (54\ amu) \rightarrow C_7H_4\ (88\ amu) + H_2\ (2\ amu) \quad (7)$$

$$C_3\ (36\ amu) + CD_2CHCHCD_2\ (58\ amu) \rightarrow C_7HD_4\ (93\ amu) + H\ \ (1\ amu) \quad (8)$$

$$C_3\ (36\ amu) + CD_2CHCHCD_2\ (58\ amu) \rightarrow C_7H_2D_3\ (92\ amu) + D\ (2\ amu) \quad (9)$$

Our analysis now concentrates on the specific site of atomic hydrogen elimination. The molecular framework of the 1,3-butadiene ($CH_2CHCHCH_2$) reactant comprises two chemically distinct classes of hydrogen atoms: four methylene hydrogens (CH_2) situated at the terminal carbon atoms (C1 and C4), and two methine hydrogens (CH) located at the central carbon atoms (C2 and C3), while tricarbon does not

https://doi.org/10.1021/acs.jpclett.5c03004
J. Phys. Chem. Lett. 2026, 17, 2942–2952

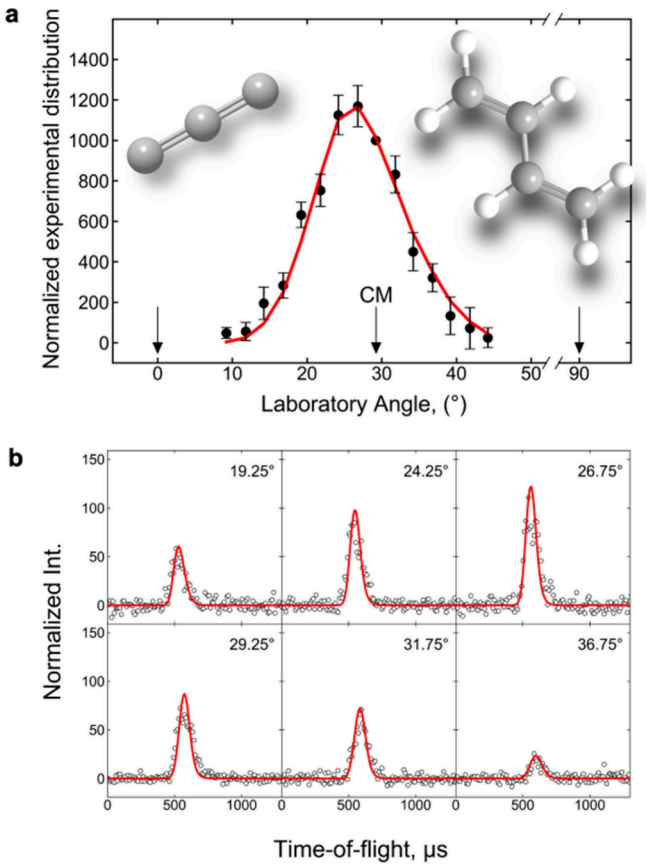

Figure 1. (a) Laboratory angular distribution and (b) time-of-flight (TOF) spectra recorded at m/z = 62 for the reaction of the tricarbon (C_3; $X^1\Sigma_g^+$) with 1,3-butadiene (C_4H_6, X^1A_g) at a collision energy of 48 ± 2 kJ mol^{-1}. The circles represent the experimental data, and the solid lines are the best fits.

possess any hydrogen atoms. This makes it sufficient to use only one partially deuterated 1,3-butadiene isotopologue, 1,3-butadiene-1,1,4,4-d_4 ($CD_2CHCHCD_2$), to study the position of the atomic hydrogen loss in the reaction. The tricarbon plus 1,3-butadiene-1,1,4,4-d_4 reaction can form C_7HD_4 (93 amu) plus H (1 amu) and/or $C_7H_2D_3$ (92 amu) plus D (2 amu). Singly ionized reaction products were monitored at m/z = 93 ($C_7HD_4^+$) and m/z = 92 ($C_7H_2D_3^+$), with reactive scattering signals detected at both mass-to-charge ratios. No signal was detected for m/z = 88 in the reaction of the tricarbon with the 1,3-butadiene fragmentation, and the molecular hydrogen loss channel does not contribute to a signal at m/z = 92 in the reaction with partially deuterated 1,3-butadiene; therefore, both the atomic hydrogen and atomic deuterium pathways are present. After integration and taking into account the dependence of the signal from the center-of-mass velocity of the scattering product, it was found that C_7HD_4 (m/z = 93) and $C_7H_2D_3$ (m/z = 92) are formed at fractions of 34 ± 1% and 66 ± 1%, respectively. Notably, the sum of the signals at m/z = 93 and 92 reproduces the signal at m/z = 89 in the reaction with 1,3-butadiene (Figure S1). The probed C_3/$CD_2CHCHCD_2$ system (reactions 8 and 9) explicitly shows that 66 ± 1% of the reaction products were formed by ejection of a deuterium atom from the terminal C1 position (CD_2) and 34 ± 1% by ejection of a hydrogen atom is from the C2 position in the diene. Therefore, the laboratory data alone expose that tricarbon (C_3) reacts with 1,3-butadiene (C_4H_6) involving at least two channels. Isotopic labeling revealed that atomic hydrogen emission occurs with approximately twice the probability from the C1 position of 1,3-butadiene compared to that from the C2 position.

For complex polyatomic systems, integrating experimental observations with electronic structure analysis and statistical calculations provides a powerful approach to elucidating the underlying reaction mechanisms and characterizing the nature of the isomer(s) formed. Exploiting a forward-convolution routine,[57-59] the laboratory data (TOFs, LADs) for the tricarbon−1,3−butadiene system were converted into the center-of-mass reference frame via a single channel fit (reaction 6) with a threshold energy to reaction of 40 kJ mol^{-1}. The best-fit CM functions are depicted in Figure 2. The error

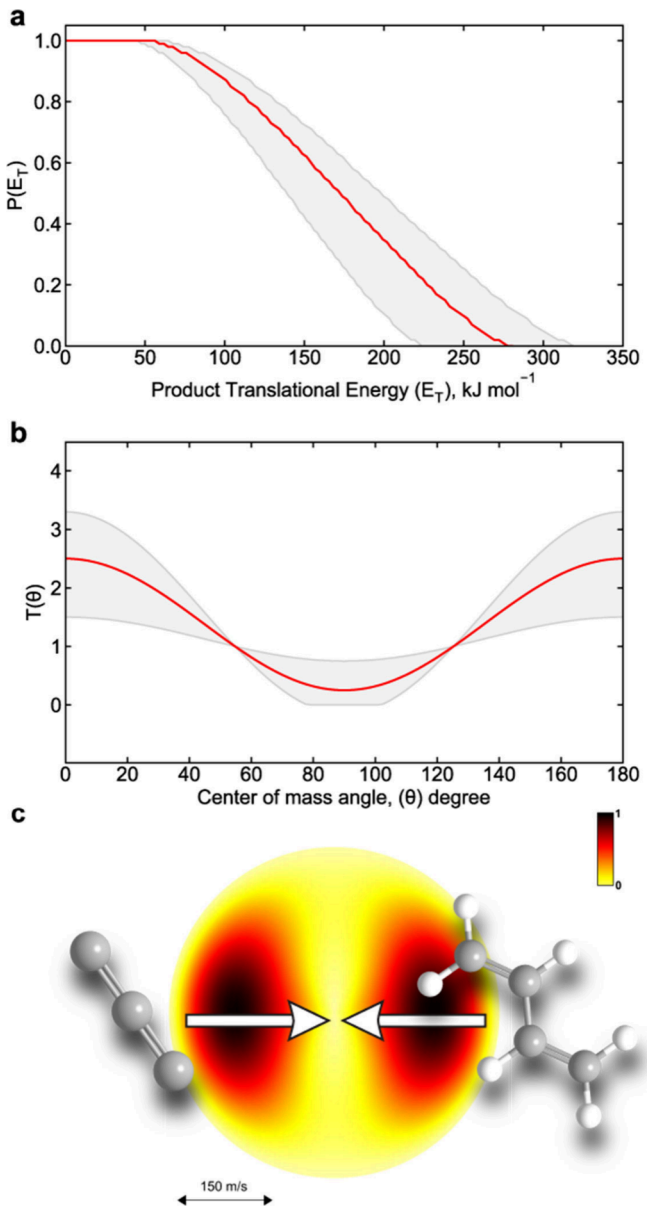

Figure 2. (a) Center-of-mass translational energy ($P(E_T)$), (b) angular distributions ($T(\theta)$), and (c) corresponding flux contour map for the reaction of the tricarbon (C_3; $X^1\Sigma_g^+$) with the 1,3-butadiene (C_4H_6, X^1A_g). For the $T(\theta)$, the direction of the C_3 beam is defined as 0° and that of the C_4H_6 as 180°. Solid lines represent the best fit, while shaded areas indicate the error limits.

https://doi.org/10.1021/acs.jpclett.5c03004
J. Phys. Chem. Lett. 2026, 17, 2942−2952

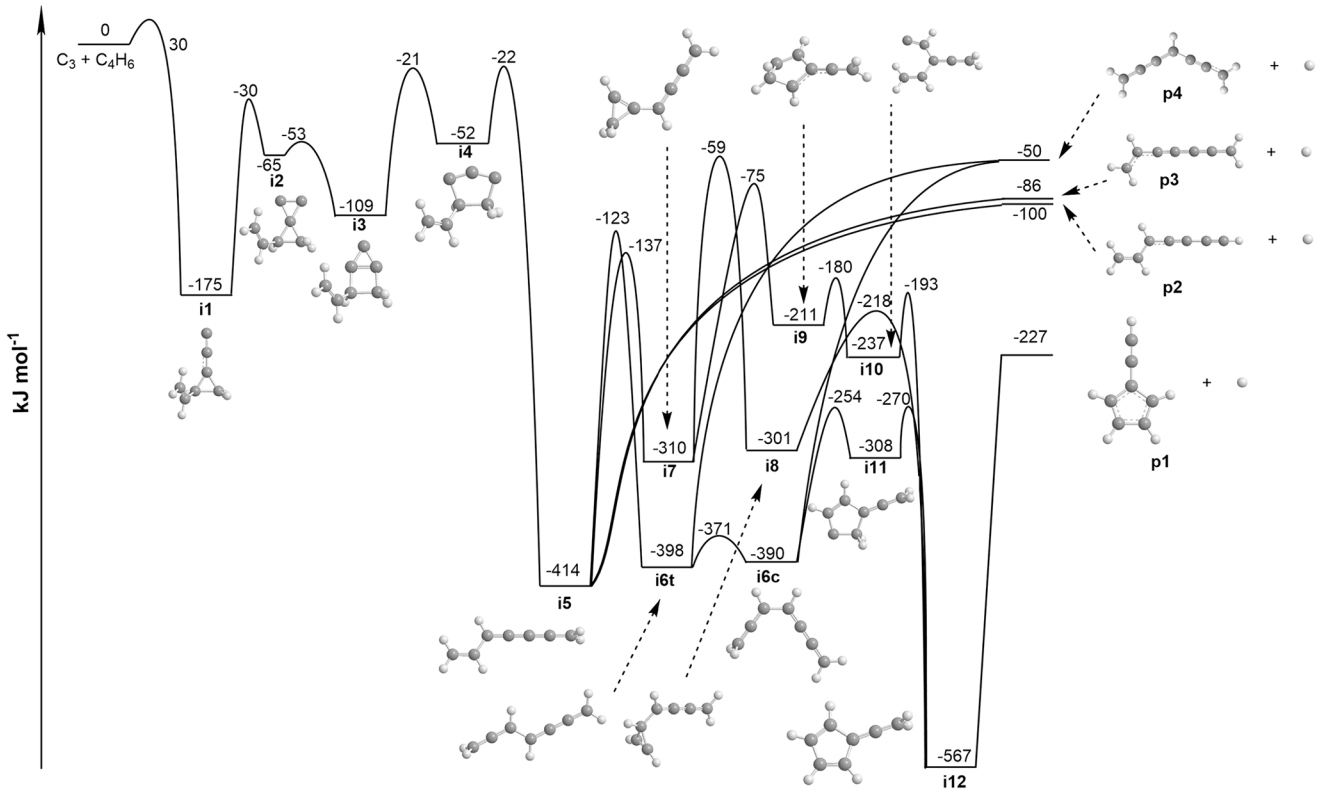

(a)

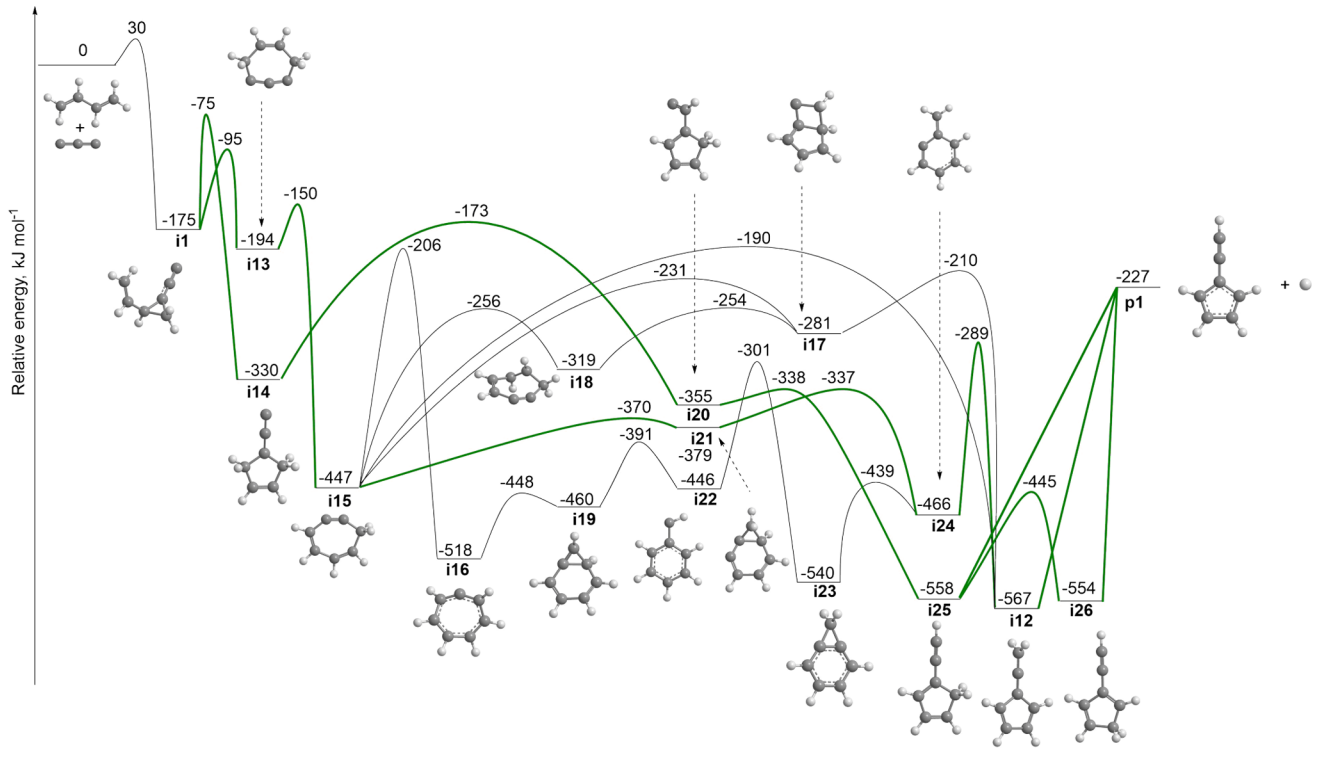

(b)

Figure 3. Potential energy surface for the bimolecular reaction of the tricarbon (C_3; $X^1\Sigma_g^+$) with the 1,3-butadiene (C_4H_6; X^1A_g) leading to C_7H_5 isomers plus the atomic hydrogen calculated at the CCSD(T)-F12/cc-pVTZ-f12//ωB97X-D/6-311G(d,p) + ZPE(ωB97X-D/6-311G(d,p)) level of theory, with the exception of structures with high T1 diagnostics, for which CASPT2(8,8) and (10,12)/cc-pVTZ were employed (see the Computational section for more details). (a) C_3 addition channels; (b) ring closure channels.

https://doi.org/10.1021/acs.jpclett.5c03004
J. Phys. Chem. Lett. 2026, 17, 2942−2952

ranges of the translational energy ($P(E_T)$) and angular flux ($T(\theta)$) functions are determined within the 1σ limits of the corresponding laboratory angular distribution and beam parameters (beam spreads, beam velocities) while maintaining a good fit of the laboratory TOF spectra and LAD. The translational energy flux distribution $P(E_T)$ (Figure 1a) offers critical insights into reaction dynamics and thermodynamics. The derived $P(E_T)$ distribution exhibits a maximum translational energy release (E_{max}) of 271 ± 47 kJ mol^{-1}. Energy conservation dictates that for those molecules born without internal excitation E_{max} is the sum of the collision energy (E_C) and the reaction exothermicity. Taking into account the collision energy of 48 ± 2 kJ mol^{-1}, the reaction energy was determined to be exoergic by 223 ± 49 kJ mol^{-1}. The $P(E_T)$ reveals a plateau starting at zero translational energy and going up to 57 ± 10 kJ mol^{-1}, suggesting that the C_7H_6 complex dissociates to C_7H_5 plus H without an exit barrier.[60] The average translational energy of the products was determined to be 93 ± 16 kJ mol^{-1}, indicating that 34 ± 12% of the total available energy is partitioned into translational degrees of freedom. This energy distribution supports a reaction mechanism involving the formation of a covalently bound C_7H_6 intermediate.[12,18,56]

The center-of-mass angular distribution $T(\theta)$ can provide additional information about the reaction dynamics (Figure 2b). The tricarbon plus 1,3-butadiene system reveals forward-backward symmetry with respect to 90°; this finding also suggests an indirect reaction mechanism involving long-lived C_7H_6 intermediate(s) that have a lifetime longer than their rotational period.[61] Finally, the maxima of the $T(\theta)$ at 0° and 180° ("coplanar scattering") highlights that at least one channel with a long-lived intermediate C_7H_6 emits a hydrogen atom in the rotational plane of the decomposing complex.[60,62] These findings are further illustrated in the flux contour map (Figure 2c), which provides a comprehensive representation of the reaction scattering process.

Now we integrate our experimental findings with electronic structure and statistical calculations to elucidate the chemical dynamics and reaction mechanisms underlying the reaction of tricarbon (C_3, $X^1\Sigma_g^+$) with 1,3-butadiene (C_4H_6, X^1A_g) in the gas phase. Computations discovered 33 reaction intermediates leading to 16 feasible, distinct products on the potential energy surfaces (PES) (Figures 3 and S2−S6). Results of Rice−Ramsperger−Kassel−Marcus (RRKM) calculations (Tables S1−S5) are compiled in the Supporting Information. The computational results indicate that the reaction commences with the addition of a tricarbon molecule, specifically through its terminal carbon atom to one of the double bonds of 1,3-butadiene. This step proceeds over an entrance barrier of 30 kJ mol^{-1} and leads to the formation of a three-membered ring intermediate (**i1**), which is stabilized by 175 kJ mol^{-1} with respect to the separated reactants. Further, the reaction can proceed via pathways analogous to those of the C_3−C_2H_4 reaction[45] (Figure 3a) or those involving a ring closure with participation of the substituent vinyl group in 1,3-butadiene as compared to ethylene (Figure 3b). In the former group of reaction channels (Figure 3a), the C_3 moiety of **i1** may add to the C1−C2 bond to the 1,3-butadiene unit, ultimately yielding **i5** via reaction sequence **i1** → **i2** → **i3** → **i4** → **i5**. Subsequently, intermediate **i5** undergoes hydrogen atom elimination via two distinct pathways: loss from the terminal methylene (CH_2) group yields **p2** (1-heptene-4,6-diyn-3-yl), while hydrogen elimination from the methine (CH) group leads to **p3** (1,3,4,5,6-heptapentaen-3-yl). Both processes proceed through barrierless exit channels and are exoergic, with associated reaction energies of −100 kJ mol^{-1} and −86 kJ mol^{-1}, respectively. Alternatively, **i5** can overcome a barrier of 277 kJ mol^{-1} to access **i7** *via* ring closure involving C4, C3, and C2 atoms from the 1,3-butadiene moiety, coupled with a [1,2] hydrogen atom shift to the carbon atom of the tricarbon moiety. Intermediate **i7** can then undergo two competitive isomerization processes commencing with either ring expansion (**i7** → **i9**) or hydrogen atom migration (**i7** → **i8**), eventually leading to the most stable intermediate on the PES − fulvenallene (**i12**; −567 kJ mol^{-1}) − via the **i7** → **i9** → **i10** → **i12** or **i7** → **i8** → **i12** pathways. The pathway initiated by a [1,3] hydrogen shift in intermediate **i5** proceeds through a 306 kJ mol^{-1} barrier, leading to the formation of 1,2,3,5,6-heptapentaene (**i6t**). The latter can be converted to its rotational isomer **i6c** via a barrier of 33 kJ mol^{-1}. Both **i6t** and **i6c** have barrier-free exit channels to the thermodynamically least stable heptapentaenyl radical: 1,2,4,5,6-heptapentaen-3-yl (**p4**; −50 kJ mol^{-1}). Alternatively, **i6c** undergoes a five-membered ring closure to **i11**, which can access the most stable C_7H_6 isomer **i12** (fulvenallene; −567 kJ mol^{-1}) via a small barrier of 44 kJ mol^{-1}. Fulvenallene (**i12**) can finally undergo unimolecular decomposition via hydrogen atom emission from the terminal methylene group to the most thermodynamically favorable product in this reaction − fulvenallenyl radical (**p1**; −227 kJ mol^{-1}) − also via a barrier-free exit channel.

As an alternative for the C_3 addition to the C=C bond, **i1** → **i2** → **i3** → **i4** → **i5**, we also considered ring closure processes initiating at **i1**. Here, a seven-membered ring closure produces **i13**, which then undergoes a 1,2-H shift from CH_2 to the neighboring bare carbon atom forming **i15**. In turn, **i15** can isomerize to fulvenallene **i12** via five different routes: (i) **i15** → **i21** → **i24** → **i12**, with the highest in energy transition state (TS) at −289 kJ mol^{-1} relative to the reactants and 158 kJ mol^{-1} above **i15**: ring contraction of the seven-membered ring to a bicyclic structure with six- and three-membered rings, followed by the three-membered ring opening and contraction of the six-membered ring to the five-membered ring in **i12**; (ii) **i15** → **i17** → **i12**, the highest TS at −210 and 237 kJ mol^{-1} relative to C_3 + C_4H_6 and **i15**, respectively: ring contraction of the seven-membered ring to a bicyclic isomer with five- and four-membered rings; (iii) **i15** → **i18** → **i17** → **i12**, with the same critical TS as in (ii), where the seven-membered ring contraction is preceded by a conformation change; (iv) **i15** → **i16** → **i19** → **i22** → **i23** → **i24** → **i12**, the highest TS at −206 and 241 kJ mol^{-1} relative to C_3 + C_4H_6 and **i15**, respectively: 1,2-H shift from CH_2 to the bare C, ring contraction to a [6+3] bicycle, three-membered ring opening, 1,3-H shift accompanied with the three-membered ring closure, another three-membered ring opening, and contraction of the six-membered ring to the five-membered ring; and (v) the direct ring contraction of the seven-membered ring of **i15** to the five-membered ring in **i12** via a barrier of 257 kJ mol^{-1} (−190 kJ mol^{-1} relative to the reactants). The initial isomer **i1** can be also subjected to a five-membered ring closure producing **i14**. The latter features two consecutive 1,2-H migrations initiating from the ring to the C_2 tail, **i14** → **i20** → **i25**, which produce 1-ethynyl-cyclopentadiene **i25** via a TS located 173 kJ mol^{-1} below the reactants. In turn, **i25** can either directly dissociate to fulvenallenyl **p1** + H or undergo another 1,2-H shift in the ring to 2-ethynyl-cyclopentadiene **i26** and then decompose to

https://doi.org/10.1021/acs.jpclett.5c03004
J. Phys. Chem. Lett. 2026, 17, 2942−2952

the same products. The absence of exit barriers on the investigated PES correlates well with the experimentally derived $P(E_T)$ distribution, which exhibits a maximum plateau that starts from 0 kJ mol^{-1}. The more complete PES (Figure S4) includes multiple isomerization pathways between cyclic (seven-, six-, and five-membered) and bicyclic structures ([6+3], [5+3], and [5+4]) and their H loss channels producing, in addition to **p1**, various cyclic and bicyclic products (Figure S6).

Which of the multiple pathways dominates the reaction?

The RRKM calculations predict that the predominant (>97%) product is the most stable C_7H_5 isomer on the PES **p1** (fulvenallenyl; −227 kJ mol^{-1}) regardless of the collision energy (Table S1). In addition, minor amounts of bicyclic C_7H_5 products **p11** [6+3] (1.1−1.3%) and **p12** [5+4] (0.3-0.5%), as well as seven-membered ring **p13** (0.3-0.6%), can also be formed (Table S1, Figures S4 and S6). The experimentally derived reaction energy of −223 ± 49 kJ mol^{-1} for the hydrogen atom loss elimination channels also supports the formation of fulvenallenyl (**p1**) under our experimental conditions, while the minor products may be masked in the lower part of the $P(E_T)$.

Considering the reaction channels, seven-membered ring closure route **i1** → **i13** exhibits the lowest barrier of 80 kJ mol^{-1} (with the TS 95 kJ mol^{-1} below the reactants), followed by five-membered ring closure route **i1** → **i14** via a 100 kJ mol^{-1} barrier. These barriers are significantly lower than those needed to be overcome in the series of steps for C_3 addition to the C=C double bond, **i1** → **i2** → **i3** → **i4** → **i5**, where the TSs lie only 21−30 kJ mol^{-1} lower in energy than those of C_3 + C_4H_6. As a result, according to RRKM calculations, the channels illustrated in Figure 3a contribute insignificantly to the overall reaction. Alternatively, the ring closure routes via **i13** and **i14** are responsible for 68% and 32% of the overall reaction flux, respectively, at zero collision energy, but their contributions nearly equalize around 50% at the experimental collision energy of 48 kJ mol^{-1} (Table S2). According to the additional RRKM calculations (Table S3), which consider only pathways originating from intermediate **i13**, the main contribution (>90%) arises from the pathway proceeding via intermediates **i21** and **i24**.

Consequently, reaction channels 10 and 11 are identified as the most dominant in the reaction mechanism, exhibiting nearly equal contributions at the studied collision energy.

$$\mathbf{i1} \rightarrow \mathbf{i13} \rightarrow \mathbf{i15} \rightarrow \mathbf{i21} \rightarrow \mathbf{i24} \rightarrow \mathbf{i12} \quad (10)$$

$$\mathbf{i1} \rightarrow \mathbf{i14} \rightarrow \mathbf{i20} \rightarrow \mathbf{i25/i26} \quad (11)$$

Complementary experiments using 1,3-butadiene-1,1,4,4-d_4 ($CD_2CHCHCD_2$) yielded additional evidence of dominant reaction channels. Analysis of the $C_3/CD_2CHCHCD_2$ experiment (reactions 8 and 9) revealed that 66 ± 1% of the products resulted from deuterium atom ejection at the terminal C1 position (CD_2), while 34 ± 1% originated from hydrogen atom loss at the C2 position. These results are consistent with the ratio of 2:1 of D vs H atoms in $C_7D_4H_2$ intermediates of the C_3 + $CD_2CHCHCD_2$ reaction. The isotope scrambling can occur via H/D migrations in **i25** and **i26** intermediates (Figure S3) where the H/D-shift barrier is much lower than the energy required for the H/D loss. According to the RRKM calculations, about 51% of **p1** is produced from **i25** or **i26** at E_{col} = 48 kJ mol^{-1} allowing both for H and D losses, whereas the remaining 49% of **p1** are formed from **i12** where only the D loss is possible, unless isotope scrambling occurred prior the formation of this intermediate. Simplified RRKM calculations taking into account the back-and-forth **i25** ⇄ **i26** isomerization gave the **p1** + D/**p1** + H ratio as 77/23 at the experimental collision energy (Table S4), slightly overestimating the experimental result. This deviation can be accounted for by considering possible H/D migrations in **i14** and **i15** also, leading to the scrambling of H and D isotopes. However, the full statistical calculations are extremely demanding due to a high combinatorial number of possible isotopomers for the C_7H_6 intermediates involved in the reaction. It is noteworthy that only the ring closure channels from **i1** (Figure 3b and S3) allow for the isotope scrambling, while those involving C_3 addition to the double C=C bond (Figures 3a and S2) do not. Therefore, the observed complete H/D isotope scrambling can be explained only by the ring closure channels.

By integrating crossed molecular beam experiments with high-level electronic structures and RRKM calculations, we have elucidated the chemical dynamics of the gas-phase reaction between tricarbon (C_3, $X^1\Sigma_g^+$) and 1,3-butadiene (C_4H_6, X^1A_g). The reaction is initiated by terminal-carbon addition of C_3 to a double bond of 1,3-butadiene, forming a three-membered ring intermediate (**i1**) stabilized by 175 kJ mol^{-1}. Subsequent seven- and five-membered ring closures in **i1** followed by (eventual) ring contraction or H migrations, respectively, lead to the predominant formation of the most thermodynamically favorable product, the fulvenallenyl radical (**p1**; −227 kJ mol^{-1}). Although the title reaction has an entrance barrier of 30 kJ mol^{-1}, RRKM calculations at collisional energies below this threshold are not directly relevant to the studied system. However, if alternative barrierless entrance channels to the C_7H_6 PES exist, such as $C_2(X^1\Sigma_g^+)$ plus C_5H_6, and lead to the formation of, e.g., **i29** (Figure S4), fulvenallenyl may still be produced under low-energy conditions.

In conclusion, statistical calculations combined with the topological features of the PES and experimental data using deuterated 1,3-butadiene-1,1,4,4-d_4 identify the ring closure channels via **i1** → **i13** and **i1** → **i14** as the primary pathways driving product formation (Figure 3b), with the **i1** → **i14** → **i20** → **i25/i26** and **i1** → **i13** → **i15** → **i21** → **i24** → **i12** routes (green on Figure 3b) most likely dominating the reaction. This assignment is corroborated by the isotopic labeling experiments, which revealed preferential deuterium loss from the terminal CD_2 group and hydrogen loss from the central CH site, consistent with H/D scrambling in cyclic intermediates that can be accessed only through ring closure. This interpretation is consistent with the center-of-mass angular distribution, which exhibits pronounced forward−backward symmetry − a diagnostic feature of long-lived reaction intermediates whose extended lifetimes permit isotopic migration prior to dissociation. The absence of exit barriers from **i12**, **i25**, and **i26** on the PES aligns with the experimentally observed $P(E_T)$ plateau near zero translational energy. These experimental observables together with a derived reaction energy of −223 ± 49 kJ mol^{-1} for the hydrogen atom loss elimination channels firmly support the computational prediction that ring closure pathways (10) and (11) dominate the formation of the fulvenallenyl radical (**p1**; −227 kJ mol^{-1}), thereby establishing a coherent picture of the reaction dynamics in which tricarbon addition initiates

https://doi.org/10.1021/acs.jpclett.5c03004
J. Phys. Chem. Lett. 2026, 17, 2942−2952

complex cyclic rearrangements culminating in barrierless hydrogen atom loss.

The substantial energy barrier of 30 kJ mol^{-1} suggests that tricarbon (C_3, $X^1\Sigma_g^+$) can undergo addition to 1,3-butadiene (C_4H_6, X^1A_g), forming resonantly stabilized C_7H_5 radicals exclusively under high-temperature conditions. Such environments include astrophysical settings such as the circumstellar envelope of IRC+10216 and interstellar shocked regions. In contrast, these reaction pathways are inaccessible under low-temperature conditions, such as cold molecular clouds and in hydrocarbon-rich atmospheres of planets and their moons, such as Titan. Ultimately, we unveiled a previously unexplored route for the formation of C_7H_5 isomers, enriching our understanding of RSFR formation during both terrestrial and cosmic chemical evolution. These findings invite further exploration into the role of small carbon clusters that drive the molecular complexity of our universe, from the flicker of a flame to the death of a star.

MATERIALS AND METHODS

Crossed Molecular Beams

The gas-phase reaction of tricarbon (C_3; $X^1\Sigma_g^+$) with the 1,3-butadiene (C_4H_6; X^1A_g) was carried out under single-collision conditions using the crossed molecular beams machine.[33,63,64] The experimental setup, data acquisition, and data processing are described elsewhere in detail.[51,65-68] Briefly, a supersonic molecular beam of tricarbon was prepared *in situ* in the primary source chamber by laser ablation (3 mJ, 266 nm, 30 Hz; Quanta-Ray) from a rotating carbon rod. The ablated species were seeded in neat carrier gas (helium, 99.9999%, Airgas) released by a Proch-Trickl pulsed valve operating at 60 Hz with a backing pressure of 4 atm. A four-slot chopper wheel located between the skimmer of the primary source and the cold shield allowed to select the segment of the pulsed tricarbon beam with a peak velocity of v_p = 1969 ± 42 m s^{-1} and speed ratio S = 3.4 ± 0.2. This beam intersected with a neat 1,3-butadiene (Aldrich Chemistry, ≥99%) pulsed molecular beam (v_p = 760 ± 20 m s^{-1}, S = 8.0 ± 0.5) perpendicularly in the reaction chamber with a mean collision energy of 48 ± 2 kJ mol^{-1}. Experiments with a partially deuterated reactant were performed using 1,3-butadiene-1,1,4,4-d_4 ($CD_2CHCHCD_2$; Cambridge Isotopes, 98% atom D) to identify the position of the hydrogen and/or deuterium loss.

The reaction products scattered from a collisional region were monitored using a triply differentially pumped (10^{-12} Torr) quadrupole mass spectrometric detector (QMS; Extrel, QC 150; 1.2 MHz) operated in the time-of-flight (TOF) mode with electron ionization (80eV, 2mA).[69] Only ions with selected mass-to-charge (m/z) pass through the quadrupole mass filter and are detected using a Daly-counter. This detector can be rotated within the plane defined by the primary and the secondary reactant beams to record angular resolved TOF spectra, which were then integrated and normalized to extract the product angular distribution in the laboratory frame (LAD) − the signal intensity of an ion with a specific m/z versus the laboratory angle. To gain information on the reaction dynamics, TOF spectra and the laboratory angular distribution (LAD) were transformed from the laboratory to the center-of-mass (CM) frame by a forward-convolution routine.[57-59] This approach initially uses a trial angular flux $T(\theta)$ and translational energy $P(E_T)$ distributions of products in the CM frame to simulate the laboratory data (TOFs and LAD). CM functions were iteratively varied until the best fit of the TOF spectra and LAD was achieved. Together, the CM functions constitute the reactive differential cross sections $I(\theta, u) \sim P(u) \times T(\theta)$, where u is the CM velocity, θ is the angle in the CM system. The reactive differential cross sections can be represented as a flux contour map that depicts the probability of the products to scatter at a specific angle (θ) with the specific kinetic energy (u). Since the reactions of tricarbon molecules with unsaturated hydrocarbons have characteristic threshold energies (E_0), we utilized an energy-dependent cross section (σ) from collisional energy (E_{coll}), by applying the line-of-center model through eq 12[60,70] in the fitting routine.

$$\sigma \sim \begin{cases} 0, & E_{coll} < E_0 \\ 1 - \dfrac{E_0}{E_{coll}}, & E_{coll} \geq E_0 \end{cases} \tag{12}$$

Computational Methods

Geometries of various stationary structures on the C_7H_6 potential energy surface (PES) involved in the C_3 + C_4H_6 reaction, such as the reactants, products, intermediates, and transition states, were optimized hybrid via density functional ωB97X-D[71] with the 6-311G(d,p) basis set. Since some of the structures on the PES may exhibit an open-shell singlet character, the unrestricted version of the method (UωB97X-D) was employed for all of them, with a stability check of the wavefunction carried out both in the beginning and in the end of geometry optimization. Such an approach ensured that each structure was optimized in the ground electronic state. The same UωB97X-D/6-311G(d,p) level of theory was used to calculate vibrational frequencies for each stationary species, following geometry optimization. The frequencies, which differ for the C_3 + $CH_2CHCHCH_2$ and C_3 + $CD_2CHCHCD_2$ reactions, were utilized in the evaluation of zero-point vibrational energy corrections (ZPE) and in the calculations of rate constants taking the isotope effect into account. To obtain chemically accurate relative energies of various species on the C_7H_6 PES, single-point energies of all optimized structures were refined using the explicitly correlated coupled cluster CCSD(T)-F12[72,73] method with Dunning's correlation-consistent cc-pVTZ-f12 basis set.[74] In general, the final CCSD(T)-F12/cc-pVTZ-f12//ωB97X-D/6-311G(d,p) + ZPE(ωB97X-D/6-311G(d,p)) relative energies are expected to be accurate within 4 kJ mol^{-1},[75] unless the wavefunction exhibits a significant multireference character. The multireference character of the wavefunction was monitored by the T1 diagnostics in the CCSD calculations. Whenever the T1 diagnostic value exceeded the 0.02 threshold, the multireference perturbation theory CASPT2 method[76,77] was employed with the active space including 8 electrons distributed on 8 orbitals and with the cc-pVTZ basis set, CASPT2(8,8)/cc-pVTZ. For critical TSs, additional multireference calculations were also performed at the CASPT2-(10,12)/cc-pVTZ level with the active space including 10 electrons distributed on 12 orbitals. The final relative energy for each multireference structure was determined as its relative energy with respect to the global C_7H_6 minimum (fulvenallene, **i12**) computed at the CASPT2(8,8) or CASPT2(10,12)/cc-pVTZ + ZPE level plus the relative energy of **i12** with respect to the initial reactants at the CCSD(T)-F12/cc-pVTZ-f12//ωB97X-D/6-311G(d,p) + ZPE-(ωB97X-D/6-311G(d,p)). Note that the computed relative energy of fulvenallene with respect to C_3 + 1,3-butadiene, −567 kJ mol^{-1}, closely matches the experimental value of −571 kJ mol^{-1} based on the enthalpies of formation of all species involved at 0 K from Active Thermochemical Tables.[78] The overall list of multireference structures includes transitions states **i3**−**i4**, **i4**−**i5**, **i8**−**i12**, and **i6c**−**i11** for the C_3 addition pathways and can be found in Figue S4 for the ring closure channels. The Gaussian 16[79] and MOLPRO 2021[80] quantum chemistry software packages were used for the *ab initio* calculations.

The Rice−Ramsperger−Kassel−Marcus (RRKM) approach[70,81,82] was used to compute energy-dependent rate constants for all unimolecular reaction steps taking place on the C_7H_6 PES starting from the **i1** intermediate where the reaction pathways begin to branch. In these calculations, the internal energy for each C_7H_6 intermediate was assumed to be equal to the sum of the collision and chemical activation energies, where the chemical activation energy is a negative of the relative energy of the species relative to the separated C_3 + C_4H_6 reactants. For the barrierless H loss reaction steps, the microcanonical variational transition state theory was used.[83] The rate constants calculations were performed utilizing our in-house Unimol code at the zero-pressure limit,[84] to reproduce the crossed molecular

https://doi.org/10.1021/acs.jpclett.5c03004
J. Phys. Chem. Lett. 2026, 17, 2942−2952

beams conditions. The RRKM-computed rate constants were used to assess the product branching ratios for unimolecular decomposition of chemically activated **i1** within steady-state approximation.[83,84]

■ ASSOCIATED CONTENT

Data Availability Statement

The data that support the findings of this study are available in the article and the Supporting Information. Additional data are available from the corresponding authors upon reasonable request.

Supporting Information

The Supporting Information is available free of charge at https://pubs.acs.org/doi/10.1021/acs.jpclett.5c03004.

Signal for the isotope labeling experiment; potential energy surface for the bimolecular reaction of the tricarbon (C_3; $X^1\Sigma_g^+$) with the 1,3-butadiene-1,1,4,4-d_4 ($CD_2CHCHCD_2$; X^1A_g); other possible C_7H_5 products not shown on the main PES; results of RRKM calculations; optimized Cartesian coordinates (Å) and vibrational frequencies (cm^{-1}) for all intermediates, transition states, reactants, and products involved (PDF)

■ AUTHOR INFORMATION

Corresponding Authors

Ralf I. Kaiser − *Department of Chemistry, University of Hawai'i at Manoa, Honolulu, Hawai'i 96822, United States;* orcid.org/0000-0002-7233-7206; Email: ralfk@hawaii.edu

Alexander M. Mebel − *Department of Chemistry and Biochemistry, Florida International University, Miami, Florida 33199, United States;* orcid.org/0000-0002-7233-3133; Email: mebela@fiu.edu

Authors

Iakov A. Medvedkov − *Department of Chemistry, University of Hawai'i at Manoa, Honolulu, Hawai'i 96822, United States;* orcid.org/0000-0003-0672-2090

Anatoliy A. Nikolayev − *Samara National Research University, Samara 443086, Russia;* orcid.org/0000-0002-1733-3704

Zhenghai Yang − *Department of Chemistry, University of Hawai'i at Manoa, Honolulu, Hawai'i 96822, United States*

Shane J. Goettl − *Department of Chemistry, University of Hawai'i at Manoa, Honolulu, Hawai'i 96822, United States;* orcid.org/0000-0003-1796-5725

Complete contact information is available at: https://pubs.acs.org/10.1021/acs.jpclett.5c03004

Author Contributions

The manuscript was written through contributions of all authors. All authors have given approval to the final version of the manuscript.

Notes

The authors declare no competing financial interest.

■ ACKNOWLEDGMENTS

The experimental studies at the University of Hawaii were supported by the US Department of Energy, Basic Energy Sciences DE-FG02-03ER15411.

■ REFERENCES

(1) Da Silva, G.; Bozzelli, J. W. The C_7H_5 Fulvenallenyl Radical as a Combustion Intermediate: Potential New Pathways to Two- and Three-Ring PAHs. *J. Phys. Chem. A* **2009**, *113* (44), 12045−12048.

(2) Zhang, T.; Zhang, L.; Hong, X.; Zhang, K.; Qi, F.; Law, C. K.; Ye, T.; Zhao, P.; Chen, Y. An Experimental and Theoretical Study of Toluene Pyrolysis with Tunable Synchrotron VUV Photoionization and Molecular-Beam Mass Spectrometry. *Combust. Flame* **2009**, *156* (11), 2071−2083.

(3) Steinbauer, M.; Hemberger, P.; Fischer, I.; Bodi, A. Photoionization of C_7H_6 and C_7H_5: Observation of the Fulvenallenyl Radical. *ChemPhysChem* **2011**, *12* (10), 1795−1797.

(4) Da Silva, G.; Trevitt, A. J. Chemically Activated Reactions on the C_7H_5 Energy Surface: Propargyl + Diacetylene, *i*-C_5H_3 + Acetylene, and *n*-C_5H_3 + Acetylene. *Phys. Chem. Chem. Phys.* **2011**, *13* (19), 8940.

(5) Frenklach, M.; Mebel, A. M. On the Mechanism of Soot Nucleation. *Phys. Chem. Chem. Phys.* **2020**, *22* (9), 5314−5331.

(6) Frenklach, M. Reaction Mechanism of Soot Formation in Flames. *Phys. Chem. Chem. Phys.* **2002**, *4* (11), 2028−2037.

(7) Marinov, N. M.; Pitz, W. J.; Westbrook, C. K.; Castaldi, M. J.; Senkan, S. M. Modeling of Aromatic and Polycyclic Aromatic Hydrocarbon Formation in Premixed Methane and Ethane Flames. *Combustion Science and Technology* **1996**, *116-117* (1-6), 211−287.

(8) Galimova, G. R.; Medvedkov, I. A.; Mebel, A. M. The Role of Methylaryl Radicals in the Growth of Polycyclic Aromatic Hydrocarbons: The Formation of Five-Membered Rings. *J. Phys. Chem. A* **2022**, *126* (7), 1233−1244.

(9) Kaiser, R. I.; Stranges, D.; Bevsek, H. M.; Lee, Y. T.; Suits, A. G. Crossed-Beam Reaction of Carbon Atoms with Hydrocarbon Molecules. IV. Chemical Dynamics of Methylpropargyl Radical Formation, C_4H_5, from Reaction of $C(^3P_j)$ with Propylene, C_3H_6 (X^1A). *J. Chem. Phys.* **1997**, *106* (12), 4945−4953.

(10) Medvedkov, I. A.; Yang, Z.; Nikolayev, A. A.; Goettl, S. J.; Eckhardt, A. K.; Mebel, A. M.; Kaiser, R. I. Binding the Power of Cycloaddition and Cross-Coupling in a Single Mechanism: An Unexpected Bending Journey to Radical Chemistry of Butadiynyl with Conjugated Dienes. *J. Phys. Chem. Lett.* **2025**, *16* (2), 658−666.

(11) Kaiser, R. I.; Hansen, N. An Aromatic Universe − A Physical Chemistry Perspective. *J. Phys. Chem. A* **2021**, *125* (18), 3826−3840.

(12) Kaiser, R. I. Experimental Investigation on the Formation of Carbon-Bearing Molecules in the Interstellar Medium via Neutral−Neutral Reactions. *Chem. Rev.* **2002**, *102* (5), 1309−1358.

(13) Kaiser, R. I.; Mebel, A. M. The Reactivity of Ground-State Carbon Atoms with Unsaturated Hydrocarbons in Combustion Flames and in the Interstellar Medium. *International Reviews in Physical Chemistry* **2002**, *21* (2), 307−356.

(14) Gu, X.; Kaiser, R. I.; Mebel, A. M. Chemistry of Energetically Activated Cumulenes—From Allene (H_2CCCH_2) to Hexapentaene ($H_2CCCCCCH_2$). *ChemPhysChem* **2008**, *9* (3), 350−369.

(15) Mebel, A. M.; Kaiser, R. I. Formation of Resonantly Stabilised Free Radicals via the Reactions of Atomic Carbon, Dicarbon, and Tricarbon with Unsaturated Hydrocarbons: Theory and Crossed Molecular Beams Experiments. *International Reviews in Physical Chemistry* **2015**, *34* (4), 461−514.

(16) Kaiser, R. I.; Balucani, N. Astrobiology − the Final Frontier in Chemical Reaction Dynamics. *International Journal of Astrobiology* **2002**, *1* (1), 15−23.

(17) Frenklach, M.; Clary, D. W.; Gardiner, W. C.; Stein, S. E. Detailed Kinetic Modeling of Soot Formation in Shock-Tube Pyrolysis of Acetylene. *Symposium (International) on Combustion* **1985**, *20* (1), 887−901.

(18) Kaiser, R. I.; Maksyutenko, P.; Ennis, C.; Zhang, F.; Gu, X.; Krishtal, S. P.; Mebel, A. M.; Kostko, O.; Ahmed, M. Untangling the Chemical Evolution of Titan's Atmosphere and Surface−from Homogeneous to Heterogeneous Chemistry. *Faraday Discuss.* **2010**, *147*, 429−478.

(19) Shiomi, T.; Nagai, H.; Kato, K.; Hiramatsu, M.; Nawata, M. Detection of C_2 Radicals in Low-Pressure Inductively Coupled Plasma

Source for Diamond Chemical Vapor Deposition. *Diamond and Related Materials* **2001**, *10* (3), 388−392.
(20) Li, W.; Wu, M.; Wang, C.; Huang, J.; Yang, J.; Xu, M.; Zhang, F.; Yang, T.; Zhao, L. Unconventional Pathway for the Gas-Phase Formation of 14π-PAHs *via* Self-Reaction of the Resonantly Stabilized Radical Fulvenallenyl ($C_7H_5^{\cdot}$). *Chem. Sci.* **2025**, *16* (18), 7864−7875.
(21) Mebel, A. M.; Li, W.; Pratali Maffei, L.; Cavallotti, C.; Morozov, A. N.; Wang, C.-Y.; Yang, J.-Z.; Zhao, L.; Kaiser, R. I. Fulvenallenyl Radical ($C_7H_5\cdot$)-Mediated Gas-Phase Synthesis of Bicyclic Aromatic $C_{10}H_8$ Isomers: Can Fulvenallenyl Efficiently React with Closed-Shell Hydrocarbons? *J. Phys. Chem. A* **2024**, *128* (28), 5707−5720.
(22) Jin, H.; Farooq, A. C7 Reaction Mechanism and Its Self-Imitation in the Kinetic Modeling of PAH Formation. *Combust. Flame* **2023**, *253*, No. 112816.
(23) Kaiser, R. I.; Stranges, D.; Lee, Y. T.; Suits, A. G. Neutral-Neutral Reactions in the Interstellar Medium. I. Formation of Carbon Hydride Radicals via Reaction of Carbon Atoms with Unsaturated Hydrocarbons. *Astrophys. J.* **1997**, *477* (2), 982.
(24) Gu, X.; Guo, Y.; Zhang, F.; Mebel, A. M.; Kaiser, R. I. Reaction Dynamics of Carbon-Bearing Radicals in Circumstellar Envelopes of Carbon Stars. *Faraday Discuss.* **2006**, *133*, 245.
(25) Kaiser, R. I.; Le, T. N.; Nguyen, T. L.; Mebel, A. M.; Balucani, N.; Lee, Y. T.; Stahl, F.; Schleyer, P. v R.; Schaefer III, H. F. A Combined Crossed Molecular Beam and Ab Initio Investigation of C_2 and C_3 Elementary Reactions with Unsaturated Hydrocarbons—Pathways to Hydrogen Deficient Hydrocarbon Radicals in Combustion Flames. *Faraday Discuss.* **2001**, *119* (0), 51−66.
(26) *Combustion Chemistry: Elementary Reactions to Macroscopic Processes: Faraday Discussion 119*, 1st ed.; Royal Society of Chemistry: London, 2001.
(27) Kern, R. D.; Xie, K.; Chen, H. A Shock Tube Study of Chlorobenzene Pyrolysis. *Combustion Science and Technology* **1992**, *85* (1-6), 77−86.
(28) Kazakov, A.; Frenklach, M. Dynamic Modeling of Soot Particle Coagulation and Aggregation: Implementation With the Method of Moments and Application to High-Pressure Laminar Premixed Flames. *Combustion and Flame* **1998**, *114* (3-4), 484−501.
(29) Ehrenfreund, P.; Charnley, S. B. Organic Molecules in the Interstellar Medium, Comets, and Meteorites: A Voyage from Dark Clouds to the Early Earth. *Annual Review of Astronomy and Astrophysics* **2000**, *38* (1), 427−483.
(30) Geppert, W. D.; Naulin, C.; Costes, M.; Capozza, G.; Cartechini, L.; Casavecchia, P.; Gualberto Volpi, G. Combined Crossed-Beam Studies of $C(^3P_j)+C_2H_4\rightarrow C_3H_3+H$ Reaction Dynamics between 0.49 and 30.8 kJ Mol^{-1}. *J. Chem. Phys.* **2003**, *119* (20), 10607−10617.
(31) Balucani, N.; Leonori, F.; Petrucci, R.; Hickson, K. M.; Casavecchia, P. Crossed Molecular Beam Studies of $C(^3P,^1D)$ and $C_2(X^1\Sigma_g^+,a^3\Pi_u)$ Reactions with Acetylene. *Phys. Scr.* **2008**, *78* (5), No. 058117.
(32) Parker, D. S. N.; Zhang, F.; Kim, Y. S.; Kaiser, R. I.; Mebel, A. M. On the Formation of Resonantly Stabilized C_5H_3 Radicals−A Crossed Beam and Ab Initio Study of the Reaction of Ground State Carbon Atoms with Vinylacetylene. *J. Phys. Chem. A* **2011**, *115* (5), 593−601.
(33) Kaiser, R. I.; Mebel, A. M.; Chang, A. H. H.; Lin, S. H.; Lee, Y. T. Crossed-Beam Reaction of Carbon Atoms with Hydrocarbon Molecules. V. Chemical Dynamics of n-C4H3 Formation from Reaction of C(3Pj) with Allene, H2CCCH2(X^1A1). *J. Chem. Phys.* **1999**, *110* (21), 10330−10344.
(34) Thomas, A. M.; Lucas, M.; Zhao, L.; Liddiard, J.; Kaiser, R. I.; Mebel, A. M. A Combined Crossed Molecular Beams and Computational Study on the Formation of Distinct Resonantly Stabilized C_5H_3 Radicals *via* Chemically Activated C_5H_4 and C_6H_6 Intermediates. *Phys. Chem. Chem. Phys.* **2018**, *20* (16), 10906−10925.
(35) Dangi, B. B.; Maity, S.; Kaiser, R. I.; Mebel, A. M. A Combined Crossed Beam and Ab Initio Investigation of the Gas Phase Reaction of Dicarbon Molecules (C_2; $X^1\Sigma_g^+/a\ ^3\Pi_u$) with Propene (C_3H_6; X^1A'): Identification of the Resonantly Stabilized Free Radicals 1- and 3-Vinylpropargyl. *J. Phys. Chem. A* **2013**, *117* (46), 11783−11793.
(36) Zhang, F.; Kim, S.; Kaiser, R. I.; Mebel, A. M. Formation of the 1,3,5-Hexatriynyl Radical ($C_6H(X^2\Pi)$) via the Crossed Beams Reaction of Dicarbon ($C_2(X^1\Sigma_g^+/a^3\Pi_u)$), with Diacetylene ($C_4H_2(X^1\Sigma_g^+)$). *J. Phys. Chem. A* **2009**, *113* (7), 1210−1217.
(37) Kaiser, R. I.; Goswami, M.; Maksyutenko, P.; Zhang, F.; Kim, Y. S.; Landera, A.; Mebel, A. M. A Crossed Molecular Beams and Ab Initio Study on the Formation of C_6H_3 Radicals. An Interface between Resonantly Stabilized and Aromatic Radicals. *J. Phys. Chem. A* **2011**, *115* (37), 10251−10258.
(38) Zhang, F.; Jones, B.; Maksyutenko, P.; Kaiser, R. I.; Chin, C.; Kislov, V. V.; Mebel, A. M. Formation of the Phenyl Radical [$C_6H_5(X^2A_1)$] under Single Collision Conditions: A Crossed Molecular Beam and Ab Initio Study. *J. Am. Chem. Soc.* **2010**, *132* (8), 2672−2683.
(39) Parker, D. S. N.; Maity, S.; Dangi, B. B.; Kaiser, R. I.; Landera, A.; Mebel, A. M. Understanding the Chemical Dynamics of the Reactions of Dicarbon with 1-Butyne, 2-Butyne, and 1,2-Butadiene − toward the Formation of Resonantly Stabilized Free Radicals. *Phys. Chem. Chem. Phys.* **2014**, *16* (24), 12150−12163.
(40) Dangi, B. B.; Parker, D. S. N.; Yang, T.; Kaiser, R. I.; Mebel, A. M. Gas-Phase Synthesis of the Benzyl Radical ($C_6H_5CH_2$). *Angew. Chem. Int. Ed.* **2014**, *53* (18), 4608−4613.
(41) Dangi, B. B.; Parker, D. S. N.; Kaiser, R. I.; Belisario-Lara, D.; Mebel, A. M. An Experimental and Theoretical Investigation of the Formation of C_7H_7 Isomers in the Bimolecular Reaction of Dicarbon Molecules with 1,3-Pentadiene. *Chemical Physics Letters* **2014**, *607*, 92−99.
(42) Balucani, N.; Mebel, A. M.; Lee, Y. T.; Kaiser, R. I. A Combined Crossed Molecular Beam and Ab Initio Study of the Reactions $C_2(X\Sigma_g^+, a^3\Pi_u) + C_2H_4 \rightarrow$ n-$C_4H_3(XA') + H(^2S^{1/2})$. *J. Phys. Chem. A* **2001**, *105* (43), 9813−9818.
(43) Kaiser, R. I.; Balucani, N.; Charkin, D. O.; Mebel, A. M. A Crossed Beam and Ab Initio Study of the $C_2(X^1\Sigma_g^+/a^3\Pi_u) + C_2H_2(X^1\Sigma_g^+)$ Reactions. *Chem. Phys. Lett.* **2003**, *382* (1-2), 112−119.
(44) Medvedkov, I. A.; Yang, Z.; Goettl, S. J.; Kaiser, R. I. Identification of the Elusive Methyl-Loss Channel in the Crossed Molecular Beam Study of Gas-Phase Reaction of Dicarbon Molecules (C_2; $X^1\Sigma_g^+/a^3\Pi_u$) with 2-Methyl-1,3-Butadiene (C_5H_8; X^1A'). *J. Phys. Chem. A* **2025**, *129* (14), 3280−3288.
(45) Gu, X.; Guo, Y.; Mebel, A. M.; Kaiser, R. I. A Crossed Beam Investigation of the Reactions of Tricarbon Molecules, $C_3(X^1\Sigma_g^+)$, with Acetylene, $C_2H_2(X_1\Sigma_g^+)$, Ethylene, $C_2H_4(X_1A_g)$, and Benzene, $C_6H_6(X^1A_{1g})$. *Chem. Phys. Lett.* **2007**, *449* (1-3), 44−52.
(46) Guo, Y.; Gu, X.; Zhang, F.; Mebel, A. M.; Kaiser, R. I. A Crossed Molecular Beam Studyon the Formation of Hexenediynyl Radicals ($H_2CCCCCH$; C_6H_3 ($X\ ^2A'$)) via Reactions ofTricarbon Molecules, C_3 ($X^1\Sigma_g^+$), with Allene (H_2CCCH_2; X^1A^1) and Methylacetylene(CH_3CCH; X^1A^1). *Phys. Chem. Chem. Phys.* **2007**, *9* (16), 1972−1979.
(47) Medvedkov, I. A.; Nikolayev, A. A.; Yang, Z.; Goettl, S. J.; Kuznetsova, A. A.; Eckhardt, A. K.; Mebel, A. M.; Kaiser, R. I. A Combined Crossed Molecular Beam and TheoreticalInvestigation of the Elementary Reaction of Tricarbon ($C_3(X^1\Sigma_g^+)$) with Diacetylene ($C_4H_2(X^1\Sigma_g^+)$): Gas Phase Formation of the Heptatriynylidyne Radical (l -$C_7H(X^2\Pi)$). *J.Phys. Chem. A* **2025**, *129* (17), 3931−3939.
(48) Polino, D.; Cavallotti, C. Fulvenallene Decomposition Kinetics. *J. Phys. Chem. A* **2011**, *115* (37), 10281−10289.
(49) Cernicharo, J.; Fuentetaja, R.; Agúndez, M.; Kaiser, R. I.; Cabezas, C.; Marcelino, N.; Tercero, B.; Pardo, J. R.; De Vicente, P. Discovery of Fulvenallene in TMC-1 with the QUIJOTE Line Survey. *A&A* **2022**, *663*, L9.
(50) Ramphal, I. A.; Shapero, M.; Haibach-Morris, C.; Neumark, D. M. Photodissociation Dynamics of Fulvenallene and the Fulvenallenyl Radical at 248 and 193 nm. *Phys. Chem. Chem. Phys.* **2017**, *19* (43), 29305−29314.
(51) Kaiser, R. I.; Hahndorf, I.; Huang, L. C. L.; Lee, Y. T.; Bettinger, H. F.; Schleyer, P. V. R.; Schaefer, H. F.; Schreiner, P. R.

https://doi.org/10.1021/acs.jpclett.5c03004
J. Phys. Chem. Lett. 2026, 17, 2942−2952

Crossed Beams Reaction of Atomic Carbon, $C(^3P_j)$, with D6-Benzene, $C_6D_6(X\ ^1A^1_g)$: Observation of the per-Deutero-1,2-Didehydro- Cycloheptatrienyl Radical, $C_7D_5(X^2B_2)$. *J. Chem. Phys.* **1999**, *110* (13), 6091−6094.
(52) Hahndorf, I.; Lee, Y. T.; Kaiser, R. I.; Vereecken, L.; Peeters, J.; Bettinger, H. F.; Schreiner, P. R.; Schleyer, P. V. R.; Allen, W. D.; Schaefer, H. F. A Combined Crossed-Beam, *Ab Initio*, and Rice−Ramsperger−Kassel− Marcus Investigation of the Reaction of Carbon Atoms $C(^3P_j)$ with Benzene, $C_6H_6(X\ ^1A^1_g)$ and d_6-Benzene, $C_6D_6(X_1A^1_g)$. *J. Chem. Phys.* **2002**, *116* (8), 3248−3262.
(53) Bettinger, H. F.; Schleyer, P. V. R.; Schaefer, H. F.; Schreiner, P. R.; Kaiser, R. I.; Lee, Y. T. The Reaction of Benzene with a Ground State Carbon Atom, $C(^3P_j)$. *J. Chem. Phys.* **2000**, *113* (10), 4250−4264.
(54) Izadi, M. E.; Bal, K. M.; Maghari, A.; Neyts, E. C. Reaction Mechanisms of $C(^3P_J)$ and $C^+(^2P_J)$ with Benzene in the Interstellar Medium from Quantum Mechanical Molecular Dynamics Simulations. *Phys. Chem. Chem. Phys.* **2021**, *23* (7), 4205−4216.
(55) Jin, H.; Xing, L.; Yang, J.; Zhou, Z.; Qi, F.; Farooq, A. Continuous Butadiyne Addition to Propargyl: A Radical-Efficient Pathway for Polycyclic Aromatic Hydrocarbons. *J. Phys. Chem. Lett.* **2021**, *12* (33), 8109−8114.
(56) Kaiser, R. I.; Mebel, A. M. On the Formation of Polyacetylenes and Cyanopolyacetylenes in Titan's Atmosphere and Their Role in Astrobiology. *Chem. Soc. Rev.* **2012**, *41* (16), 5490.
(57) Vernon, M. F. Molecular Beam Scattering. Ph.D. Dissertation, University of California: Berkeley, CA, 1983.
(58) Weiss, P. S. *Reaction Dynamics of Electronically Excited Alkali Atoms with Simple Molecules*, Ph.D. Dissertation, University of California: Berkeley, CA, 1986.
(59) Kaiser, R. I.; Ochsenfeld, C.; Stranges, D.; Head-Gordon, M.; Lee, Y. T. Combined Crossed Molecular Beams and Ab Initio Investigation of the Formation of Carbon-Bearing Molecules in the Interstellar Medium via Neutral−Neutral Reactions. *Faraday Discuss.* **1998**, *109* (0), 183−204.
(60) Levine, R. D. *Molecular Reaction Dynamics*; Cambridge University Press: Cambridge, UK, 2005.
(61) Levine, R. D. *Molecular Reaction Dynamics*, paperback ed.; Cambridge University Press: Cambridge, 2009.
(62) Miller, W. B.; Safron, S. A.; Herschbach, D. R. Exchange Reactions of Alkali Atoms with Alkali Halides: A Collision Complex Mechanism. *Discuss. Faraday Soc.* **1967**, *44*, 108.
(63) Huang, L. C. L.; Balucani, N.; Lee, Y. T.; Kaiser, R. I.; Osamura, Y. Crossed Beam Reaction of the Cyano Radical, $CN(X^2\Sigma^+)$, with Methylacetylene, CH_3CCH (X^1A^1): Observation of Cyanopropyne, CH_3CCCN (X^1A^1), and Cyanoallene, $H_2CCCHCN$ (X^1A'). *J. Chem. Phys.* **1999**, *111* (7), 2857−2860.
(64) Stahl, F.; von Ragué Schleyer, P.; Bettinger, H. F.; Kaiser, R. I.; Lee, Y. T.; Schaefer, H. F. III. Reaction of the Ethynyl Radical, C_2H, with Methylacetylene, CH3CCH, under Single Collision Conditions: Implications for Astrochemistry. *The Journal of Chemical Physics* **2001**, *114* (8), 3476−3487.
(65) Kaiser, R. I.; Parker, D. S. N.; Zhang, F.; Landera, A.; Kislov, V. V.; Mebel, A. M. PAH Formation under Single Collision Conditions: Reaction of Phenyl Radical and 1,3-Butadiene to Form 1,4-Dihydronaphthalene. *J. Phys. Chem. A* **2012**, *116* (17), 4248−4258.
(66) Medvedkov, I. A.; Nikolayev, A. A.; Goettl, S. J.; Yang, Z.; Mebel, A. M.; Kaiser, R. I. Experimental and Theoretical Study of the Sn−O Bond Formation between Atomic Tin and Molecular Oxygen. *Phys. Chem. Chem. Phys.* **2024**, *26* (43), 27763−27771.
(67) Maksyutenko, P.; Zhang, F.; Gu, X.; Kaiser, R. I. A Crossed Molecular Beam Study on the Reaction of Methylidyne Radicals $[CH(X^2\Pi)]$ with Acetylene $[C_2H_2\ (X^1\Sigma_g^+)]$−Competing C_3H_2 + H and C_3H + H_2 Channels. *Phys. Chem. Chem. Phys.* **2011**, *13* (1), 240−252.
(68) Stahl, F.; Schleyer, P. v. R.; Schaefer III, H. F.; Kaiser, R. I. Reactions of Ethynyl Radicals as a Source of C4 and C5 Hydrocarbons in Titan's Atmosphere. *Planetary and Space Science* **2002**, *50* (7-8), 685−692.
(69) Daly, N. R. Scintillation Type Mass Spectrometer Ion Detector. *Review of Scientific Instruments* **1960**, *31* (3), 264−267.
(70) Steinfeld, J. I.; Francisco, J. S.; Hase, W. L. *Chemical Kinetics and Dynamics*, 2nd ed.; Pearson: Upper Saddle River, NJ, 1998.
(71) Chai, J.-D.; Head-Gordon, M. Long-Range Corrected Hybrid Density Functionals with Damped Atom−Atom Dispersion Corrections. *Phys. Chem. Chem. Phys.* **2008**, *10* (44), 6615−6620.
(72) Knizia, G.; Adler, T. B.; Werner, H.-J. Simplified CCSD(T)-F12 Methods: Theory and Benchmarks. *The Journal of Chemical Physics* **2009**, *130* (5), No. 054104.
(73) Adler, T. B.; Knizia, G.; Werner, H.-J. A Simple and Efficient CCSD(T)-F12 Approximation. *The Journal of Chemical Physics* **2007**, *127* (22), No. 221106.
(74) Dunning, T. H., Jr. Gaussian Basis Sets for Use in Correlated Molecular Calculations. I. The Atoms Boron through Neon and Hydrogen. *The Journal of Chemical Physics* **1989**, *90* (2), 1007−1023.
(75) Zhang, J.; Valeev, E. F. Prediction of Reaction Barriers and Thermochemical Properties with Explicitly Correlated Coupled-Cluster Methods: A Basis Set Assessment. *J. Chem. Theory Comput.* **2012**, *8* (9), 3175−3186.
(76) Celani, P.; Werner, H.-J. Multireference Perturbation Theory for Large Restricted and Selected Active Space Reference Wave Functions. *The Journal of Chemical Physics* **2000**, *112* (13), 5546−5557.
(77) Shiozaki, T.; Györffy, W.; Celani, P.; Werner, H.-J. Communication: Extended Multi-State Complete Active Space Second-Order Perturbation Theory: Energy and Nuclear Gradients. *The Journal of Chemical Physics* **2011**, *135* (8), No. 081106.
(78) Ruscic, B.; Bross, D. H. *Active Thermochemical Tables (ATcT) Values Based on Ver. 1.220 of the Thermochemical Network*; Argonne National Laboratory: Lemont, Illinois, USA, 2025; available at atct.anl.gov DOI: 10.17038/CSE/2568691.
(79) Frisch, M. J.; Trucks, G. W.; Schlegel, H. B.; Scuseria, G. E.; Robb, M. A.; Cheeseman, J. R.; Scalmani, G.; Barone, V.; Petersson, G. A.; Nakatsuji, H.; Li, X.; Caricato, M.; Marenich, A. V.; Bloino, J.; Janesko, B. G.; Gomperts, R.; Mennucci, B.; Hratchian, H. P.; Ortiz, J. V.; Izmaylov, A. F.; Sonnenberg, J. L.; Williams; Ding, F.; Lipparini, F.; Egidi, F.; Goings, J.; Peng, B.; Petrone, A.; Henderson, T.; Ranasinghe, D.; Zakrzewski, V. G.; Gao, J.; Rega, N.; Zheng, G.; Liang, W.; Hada, M.; Ehara, M.; Toyota, K.; Fukuda, R.; Hasegawa, J.; Ishida, M.; Nakajima, T.; Honda, Y.; Kitao, O.; Nakai, H.; Vreven, T.; Throssell, K.; Montgomery, J. A., Jr.; Peralta, J. E.; Ogliaro, F.; Bearpark, M. J.; Heyd, J. J.; Brothers, E. N.; Kudin, K. N.; Staroverov, V. N.; Keith, T. A.; Kobayashi, R.; Normand, J.; Raghavachari, K.; Rendell, A. P.; Burant, J. C.; Iyengar, S. S.; Tomasi, J.; Cossi, M.; Millam, J. M.; Klene, M.; Adamo, C.; Cammi, R.; Ochterski, J. W.; Martin, R. L.; Morokuma, K.; Farkas, O.; Foresman, J. B.; Fox, D. J. *Gaussian 16*; Gaussian, 2016.
(80) Werner, H.-J.; Knowles, P. J.; Celani, P.; Györffy, W.; Hesselmann, A.; Kats, D.; Knizia, G.; Köhn, A.; Korona, T.; Kreplin, D.; Lindh, R.; Ma, Q.; Manby, F. R.; Mitrushenkov, A.; Rauhut, G.; Schütz, M.; Shamasundar, K. R.; Adler, T. B.; Amos, R. D.; Bennie, S. J.; Bernhardsson, A.; Berning, A.; Black, J. A.; Bygrave, P. J.; Cimiraglia, R.; Cooper, D. L.; Coughtrie, D.; Deegan, M. J. O.; Dobbyn, A. J.; Doll, K.; Dornbach, M.; Eckert, F.; Erfort, S.; Goll, E.; Hampel, C.; Hetzer, G.; Hill, J. G.; Hodges, M.; Hrenar, T.; Jansen, G.; Köppl, C.; Kollmar, C.; Lee, S. J. R.; Liu, Y.; Lloyd, A. W.; Mata, R. A.; May, A. J.; Mussard, B.; McNicholas, S. J.; Meyer, W.; Iii, T. F. M.; Mura, M. E.; Nicklass, A.; O'Neill, D. P.; Palmieri, P.; Peng, D.; Peterson, K. A.; Pflüger, K.; Pitzer, R.; Polyak, I.; Reiher, M.; Richardson, J. O.; Robinson, J. B.; Schröder, B.; Schwilk, M.; Shiozaki, T.; Sibaev, M.; Stoll, H.; Stone, A. J.; Tarroni, R.; Thorsteinsson, T.; Toulouse, J.; Wang, M.; Welborn, M.; Ziegler, B. *MOLPRO*, Version 2021.2, a Package of Ab Initio Programs, 2021.
(81) Robinson, P. J.; Holbrook, K. A. *Unimolecular Reactions*; John Wiley and Sons: New York, 1972.
(82) Eyring, H.; Lin, S. H.; Lin, S. M. *Basic Chemical Kinetics*; John Wiley and Sons: New York, 1980.

https://doi.org/10.1021/acs.jpclett.5c03004
J. Phys. Chem. Lett. 2026, 17, 2942−2952

(83) Kislov, V. V.; Nguyen, T. L.; Mebel, A. M.; Lin, S. H.; Smith, S. C. Photodissociation of Benzene under Collision-Free Conditions: An Ab Initio/Rice−Ramsperger−Kassel−Marcus Study. *J. Chem. Phys.* **2004**, *120* (15), 7008−7017.

(84) He, C.; Zhao, L.; Thomas, A. M.; Morozov, A. N.; Mebel, A. M.; Kaiser, R. I. Elucidating the Chemical Dynamics of the Elementary Reactions of the 1-Propynyl Radical (CH_3CC; X^2A_1) with Methylacetylene (H_3CCCH; X^1A_1) and Allene (H_2CCCH_2; X^1A_1). *J. Phys. Chem. A* **2019**, *123* (26), 5446−5462.

https://doi.org/10.1021/acs.jpclett.5c03004
J. Phys. Chem. Lett. 2026, 17, 2942−2952